

# Zonal Organization of the Mouse Flocculus: Physiology, Input, and Output

MARTIJN SCHONEWILLE, CHONGDE LUO, TOM J. H. RUIGROK, JAN VOOGD,  
MATTHEW T. SCHMOLESKY, MANDY RUTTEMAN, FREEK E. HOEBEEK,  
MARCEL T. G. DE JEU, AND CHRIS I. DE ZEEUW\*

Department of Neuroscience, Erasmus MC, 3000 DR Rotterdam, The Netherlands

## ABSTRACT

The zones of the flocculus have been mapped in many species with a noticeable exception, the mouse. Here, the functional map of the mouse was constructed via extracellular recordings followed by tracer injections of biotinylated-dextran-amine and immunohistochemistry for heat-shock protein-25. Zones were identified based on the Purkinje cell complex spike modulation occurring in response to optokinetic stimulation. In zones 1 and 3 Purkinje cells responded best to rotation about a horizontal axis oriented at 135° ipsilateral azimuth, whereas in zones 2 and 4 they responded best to rotation about the vertical axis. The tracing experiments showed that Purkinje cells of zone 1 projected to the parvicellular part of lateral cerebellar nucleus and superior vestibular nucleus, while Purkinje cells of zone 3 projected to group Y and the superior vestibular nucleus. Purkinje cells of zones 2 and 4 projected to the magnocellular and parvicellular parts of the medial vestibular nucleus, while some also innervated the lateral vestibular nucleus or nucleus prepositus hypoglossi. The climbing fiber inputs to Purkinje cells in zones 1 and 3 were derived from neurons in the ventrolateral outgrowth of the contralateral inferior olive, whereas those in zones 2 and 4 were derived from the contralateral caudal dorsal cap. Purkinje cells in zones 1 and 2, but not in zones 3 and 4, were positively labeled for heat-shock protein-25. The present study illustrates that Purkinje cells in the murine flocculus are organized in discrete zones with specific functions, specific input — output relations, and a specific histochemical signature. *J. Comp. Neurol.* 497:670–682, 2006. © 2006 Wiley-Liss, Inc.

**Indexing terms:** compensatory eye movements; vestibular reference frames; optokinetic; semicircular canals; cerebellum; biotinylated-dextran-amine

The flocculus of the cerebellum plays an important role in the control of compensatory eye movements (De Zeeuw et al., 2004). The anatomical and/or physiological zones of the flocculus have been mapped for various species, including monkey (Lisberger and Fuchs, 1978), cat (Groenewegen and Voogd, 1977), rabbit (De Zeeuw et al., 1994a; Van der Steen et al., 1994; Tan et al., 1995a), and rat (Ruigrok et al., 1992; Sugihara et al., 2004). The organization of the flocculus in mammals generally follows that of the cerebellar cortex in that sagittal zones of Purkinje cells project to specific parts of the cerebellar and vestibular nuclei (Yamamoto et al., 1978; Voogd and Bigaré, 1980; Sato et al., 1982a,b; Tan et al., 1995a; Balaban et al., 2000; Sugihara et al., 2004) and that they receive their climbing fibers from a specific group of neurons in the contralateral inferior olive (IO; Groenewegen and Voogd, 1977; Groenewegen et al., 1979; Ruigrok et al., 1992; Tan et al., 1995c; Sugihara et al., 2004). In most mammals the zones can be morphologically discriminated by using ace-

tylcholinesterase staining as a biochemical marker and/or by tracing the climbing fiber inputs anterogradely from the olive (Voogd and Bigaré, 1980; Tan et al., 1995c). To date, little is known about the floccular organization in the mouse; so far no biochemical marker has been correlated

Grant sponsor: the Dutch Organization for Medical Sciences (NWO-PIONIER and ZON-MW); Grant sponsor: Life Sciences (NWO-ALW); Grant sponsor: Neuro-Bsik consortium (Senter); Grant sponsor: European Community (EC).

M. Schonewille and C. Luo contributed equally to this work.

\*Correspondence to: M. Schonewille, Department of Neuroscience, Erasmus MC, 3000 DR Rotterdam, The Netherlands. E-mail: m.schonewille@erasmusmc.nl

Received 27 June 2005; Revised 8 November 2005; Accepted 17 March 2006

DOI 10.1002/cne.21036

Published online in Wiley InterScience (www.interscience.wiley.com).

to their zones and the topography of their climbing fiber projections has not been elucidated.

Climbing fibers potentials evoke complex spikes in Purkinje cells of the cerebellar cortex (Eccles et al., 1966; Thach, 1967). In the flocculus of both rabbits and mice, the complex spike activity of Purkinje cells is modulated optimally in response to rotational optokinetic stimulation about either the vertical axis (VA) or the horizontal axis (HA) that is approximately perpendicular to the ipsilateral anterior semicircular canal (Graf et al., 1988; Goossens et al., 2004; Hoebeek et al., 2005). In zones 1 and 3 of the rabbit flocculus, complex spike activity is optimally modulated in response to optokinetic stimulation about the HA oriented at 45° contralateral azimuth/135° ipsilateral azimuth, while complex spike activities of Purkinje cells in zones 2 and 4 are optimally modulated in response to optokinetic stimulation about the vertical axis (De Zeeuw et al., 1994a). Whether the distribution of Purkinje cells with different preferred axes of optokinetic modulation in mice follows the same zonal pattern as in rabbits is unknown.

Purkinje cells in the flocculus are known to project to various parts of the cerebellar and vestibular nuclei, as demonstrated in primate (Haines, 1977; Langer et al., 1985), cat (Voogd, 1964; McCreary et al., 1979; Sato et al., 1982a), rabbit (Alley, 1977; Yamamoto and Shimoyama, 1977; Balaban, 1987), and rat (Balaban et al., 2000). These studies used degeneration and/or tracing of large groups of axons, mostly of multiple zones. Until recently

studies on the efferent projection of individual zones of the flocculus were mostly done with retrograde axonal labeling from injections in the vestibular nuclei (Yamamoto et al., 1978; Sato et al., 1982b; Tan et al., 1995a) and therefore did not provide detailed information on the precise termination of the Purkinje cell axons. The only study using anterograde axonal transport from discrete injections of individual Purkinje cells is the study by De Zeeuw and colleagues (1994a). However, the Purkinje cell projections from this study could not be directly correlated to the specific olivary origins of the climbing fiber inputs to the flocculus due to the use of biocytin, which is exclusively an anterograde tracer.

To overcome this limitation, as well as to find out whether and how the flocculus of the mouse is organized in zones, we placed small injections of biotinylated-dextran-amine (BDA), which acts as both an anterograde and a retrograde tracer, into areas that were identified electrophysiologically by recording climbing fiber responses of Purkinje cells during optokinetic stimulation. Although this technique is not as accurate as intra- or juxtacellular injections in Purkinje cells, it closely approaches this level, and in addition it labeled small areas of Purkinje cells as well as their climbing fiber inputs, thus allowing us to trace both the afferent and efferent projections of identified floccular zones in the same experiment. In addition, we investigated to what extent immunoreactivity for heat-shock protein-25 (HSP-25), which has recently been demonstrated to reveal distinct bands in the vestibulocerebellum of mice (Armstrong et al., 2000), could be correlated to the physiological identity and projection pattern of these zones. Thus in conjunction, the current study provides a full description of the anatomical and physiological organization of the flocculus of the mouse, which nowadays with the advent of transgenics, is the first mammal of choice.

#### Abbreviations

4V	4th ventricle
6	abducens nucleus
7n	facial nerve
8n	vestibulocochlear nerve
AChE	acetylcholinesterase
BDA	biotinylated dextran amine
CDC	caudal dorsal cap
Co	cochlear nucleus
DC	dorsal cap
Fl	flocculus
HA	horizontal axis
HSP-25	heat-shock protein-25
icp	inferior cerebellar peduncle
IntA	anterior interposed nucleus of the cerebellum
IntP	posterior interposed nucleus of the cerebellum
IO	inferior olive
Lat	lateral cerebellar nucleus
LatPC	parvicellular part of lateral cerebellar nucleus
LC	locus coeruleus
LVN	lateral vestibular nucleus
mcp	middle cerebellar peduncle
Me5	mesencephalic trigeminal nucleus
Med	medial cerebellar nucleus
MVe	medial vestibular nucleus
MVem	magnocellular part of medial vestibular nucleus
MVep	parvicellular part of medial vestibular nucleus
OKR	optokinetic reflex
PAG	periaqueductal gray
PFl	paraflocculus
PrH	nucleus prepositus hypoglossi
RDC	rostral dorsal cap
scp	superior cerebellar peduncle
SuVe	superior vestibular nucleus
VA	vertical axis
VLO	ventrolateral outgrowth
VOR	vestibulo-ocular reflex
vsc	ventral spinocerebellar tract
WGA-HRP	wheat germ agglutinated horseradish peroxidase

## MATERIAL AND METHODS

All procedures adhered to the NIH Guide for the Care and Use of Laboratory Animals according to the principles expressed in the declaration of Helsinki and were approved by a national committee overseeing animal welfare.

### Surgery

Eighteen adult C57BL/6 mice were prepared for neurophysiological experiments under anesthesia consisting of a 1:2 mixture of O<sub>2</sub>, N<sub>2</sub>O, and 1.5% isoflurane. An acrylic head fixation pedestal was fixed to the skull by M1 screws, and a recording chamber was made following a craniotomy (diameter ~ 3 mm) of the left occipital bone (Goossens et al., 2001). The animals were allowed to recover for 5 days before the start of the recording and injection sessions.

### Recordings and injections

The animals were restrained in a custom-made plastic tube, which was placed in the center of a random dotted drum that could be rotated around a variety of vertical or horizontal axes in space (Stahl et al., 2000; van Alphen et al., 2001). Extracellular Purkinje cell activity was recorded using filament containing borosilicate glass pipettes (OD 2.0 mm, ID 1.16 mm, tip diameter 2.0 μm) filled with 2M NaCl. For amplification, data acquisition,

and analysis, we used Cyberamp (CED, Cambridge, U.K.), Spike 2 software (CED), and custom-written Matlab routines (Mathworks), respectively. Optokinetic stimulation consisted of a full-field random-dotted black and white drum (dot size 2°, distance to head 45 cm) rotating sinusoidally with 5° amplitude at 0.4 Hz around both the VA and the HA that is perpendicular to the ipsilateral anterior semicircular canal (at a 45° angle clockwise from the rostrocaudal midline). A floccular zone was identified by its complex spike responses to this optokinetic stimulation (De Zeeuw et al., 1994a); for tuning curves in mice see (Hoebeek et al., 2005), and subsequently the recording pipette was exchanged for a pipette (tip diameter 2 μm) that was filled with 10% BDA. After the floccular zone was re-identified based on the complex spike modulation recorded with the BDA pipette, an iontophoretic injection was made using a constantly monitored anodal current of 1 to 4 μA, pulsed 7 seconds on, 7 seconds off, for a period of 10 minutes. Following the injection, the brain was covered with gramicidin-containing ointment and sealed with bone wax (Hoebeek et al., 2005).

### Tissue processing

After 5 to 7 days the mice were deeply anesthetized with pentobarbital (200 mg/kg) and perfused transcardially with 4% paraformaldehyde. The brains were postfixed for 1 hour in 4% paraformaldehyde, embedded in gelatin (11%), and sectioned transversally at 40 μm with a freezing microtome. Sections were serially collected in four glass vials in which subsequent rinsing and incubation procedures were performed. Vials 1 and 3 were incubated for both BDA and HSP-25 staining, whereas vials 2 and 4 only served for BDA histochemistry. All sections were rinsed for 30 minutes in Tris-buffered saline (TBS, pH 7.6), incubated for 90 minutes in a solution of TBS/0.05% Triton-X100/10% normal horse serum to block nonspecific protein-binding sites, incubated overnight at 4°C in avidin-biotin-peroxidase complex (Vector Laboratories, Inc., Burlingame, CA), rinsed again, and finally incubated in diaminobenzidine (75 mg/100 ml). In vials 1 and 3, cobalt ions were added to the incubation bath in order to obtain a black reaction product. The reaction was stopped after 15 to 20 minutes by rinsing in TBS. Vials 1 and 3 were subsequently incubated with the rabbit-anti-mouse HSP-25 antibody (1:10,000, SPA-801, StressGen, Victoria, BC, Canada) diluted in TBS containing 0.5% Triton-X100 and 2% normal serum. After 48 hours incubation in the dark at 4°C, the sections were rinsed in TBS (3 times) and then incubated 90 minutes with the secondary antibody biotinylated goat-anti-rabbit antibody (1:200, Vector Laboratories). After this incubation, the sections were rinsed in TBS for 60 minutes, and incubated again 90 minutes with the avidin-biotin-complex (Vector Laboratories, Inc.) in TBS with 0.5% Triton-X100. This step was followed by 3 × 5 minute rinsing in TBS and 3 × 5 minutes in 0.1M Tris buffer (pH 7.6). This time, the complex was visualized by diaminobenzidine (DAB, 75 mg/100 ml) only, thus resulting in a brown precipitate at places where HSP-25 was present. Sections of vials 2 and 4, in which only BDA was visualized as a brown precipitate, served as additional sections for analysis and plotting. The sections were mounted, air-dried, counterstained with thionin, dehydrated through graded alcohol series, cleared in xylene, and cover-slipped with Permount (Fisher Scientific). The HSP-25 antibody used in this study was generated against

recombinant mouse HSP-25. The specificity for HSP-25 has been extensively tested through preadsorption with recombinant HSP-25 and comparison with HSP-25 mRNA distribution in murine fixed brain sections in previous studies (Maatkamp et al., 2004). Furthermore, the same results were obtained with goat polyclonal antibody raised against the C-terminal portion of human HSP27, the human orthologue of HSP-25. Consistent with previous studies, both antibodies predominantly stained motoneurons in spinal cord and brainstem, and to lesser degree astrocytes and blood vessels (Maatkamp et al., 2004).

### Histological analysis

The histological material was analyzed with a Leica DMR light microscope equipped with a DC 300 digital camera. Photo panels were constructed in CorelDraw after some correction for brightness and contrast in Corel Photo-Paint (both ver. 11). Graphical plots of anterograde and retrograde labeling in the cerebellar and vestibular nuclei were made with an Olympus BH-2 microscope equipped with a Lucivid miniature monitor (Microbrightfield, Colchester, VT) and a motorized *x*, *y*, and *Z* stage drive, and Neurolucida software (Microbrightfield). Similar plots were made of retrograde labeling within the inferior olivary complex from which a standardized diagram was prepared of the caudal inferior olivary nucleus (Ruigrok et al., 1992). Olivary labeling was subsequently entered within this standardized diagram. To map the flocculus, digital prints were prepared of all consecutive sections from the caudal-most to the rostral-most part of the flocculus. In all sections four reference points were indicated which served to construct a map of the unfolded flocculus (Ruigrok et al., 1992; Balaban et al., 2000; see also Fig. 3). The unfolded flocculus map was transformed by custom-written Matlab routines.

## RESULTS

### Purkinje cell recordings and injections

Most of the complex spike activities of the Purkinje cells in the flocculus of the mouse responded optimally to optokinetic stimulation along either the VA or the HA perpendicular to the ipsilateral anterior semicircular canal (Fig. 1). In all these cases the simple spikes modulated out of phase with respect to the complex spike activities (Fig. 1C,D). The 18 small BDA injections that were made were distributed throughout the entire caudal-rostral and medio-lateral extent of the areas in the flocculus that responded to optokinetic stimulation (Figs. 2, 3). The cells that modulated optimally to the HA were clustered either in a zone located caudally in the flocculus (referred to as zone 1) or in a zone located in its rostral half (referred to as zone 3; see Fig. 3D,E). In contrast, the VA cells were all located in between or rostrally to these zones (referred to as zone 2 and zone 4). Caudal to zone 1, no cells were found that responded to optokinetic stimulation; in this area, which probably corresponds to the C2-zone (see De Zeeuw et al., 1994a; De Zeeuw and Koekkoek, 1997), no injections were made. Among the 18 BDA injections that were made in the floccular areas that showed responses to optokinetic stimulation, 4 were made into zone 1, 8 in zone 2, 5 in zone 3, and 1 in zone 4 (Table 1). Two of these injections, that is, nr 17770-8 in zone 1 and nr 15733-1 in zone 3, extended somewhat into the ventral paraflocculus. A large part of

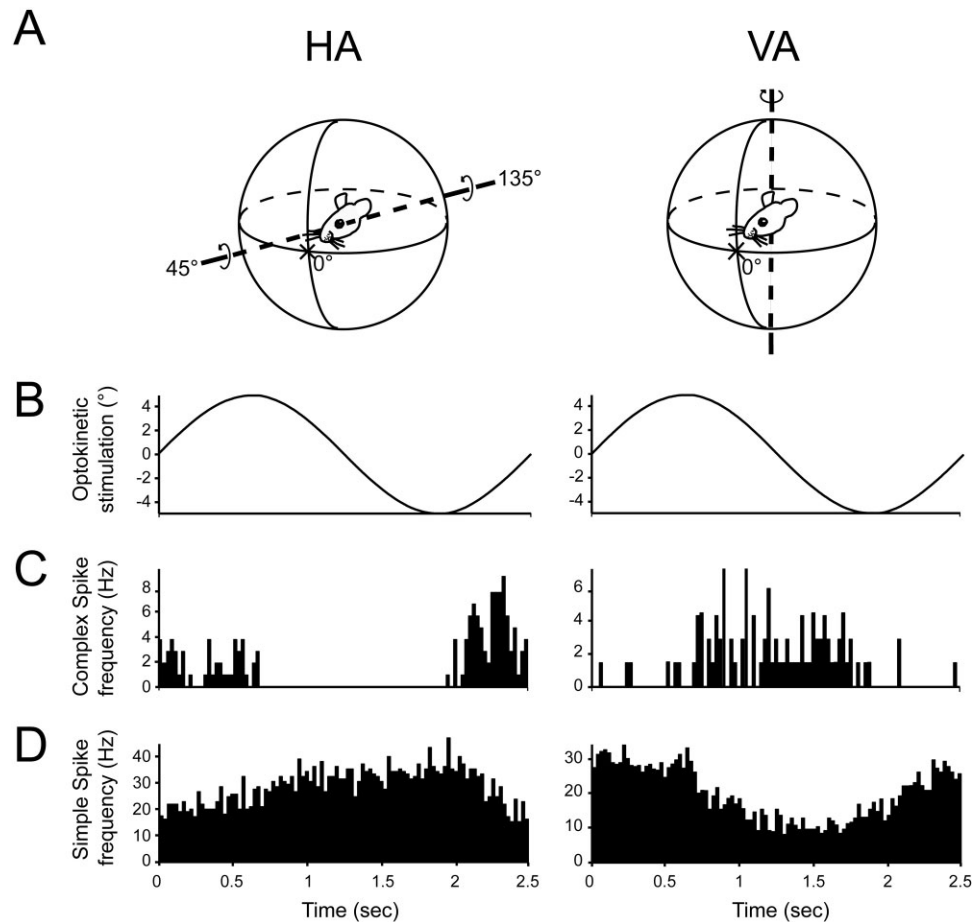


Fig. 1. Complex spike and simple spike activities of Purkinje cells in the flocculus are modulated by HA or VA visual field rotation. (A) This panel shows the spatial orientation of the optokinetic stimulation used to determine the preferred axis for each Purkinje cell. The visual field was rotated around the ipsilateral 135° posterior/contralateral 45° anterior axis in the horizontal plane (HA; left column) or the vertical axis (VA; right column). Arrows in A indicate the direction of rotation that results in increased complex spike activity in

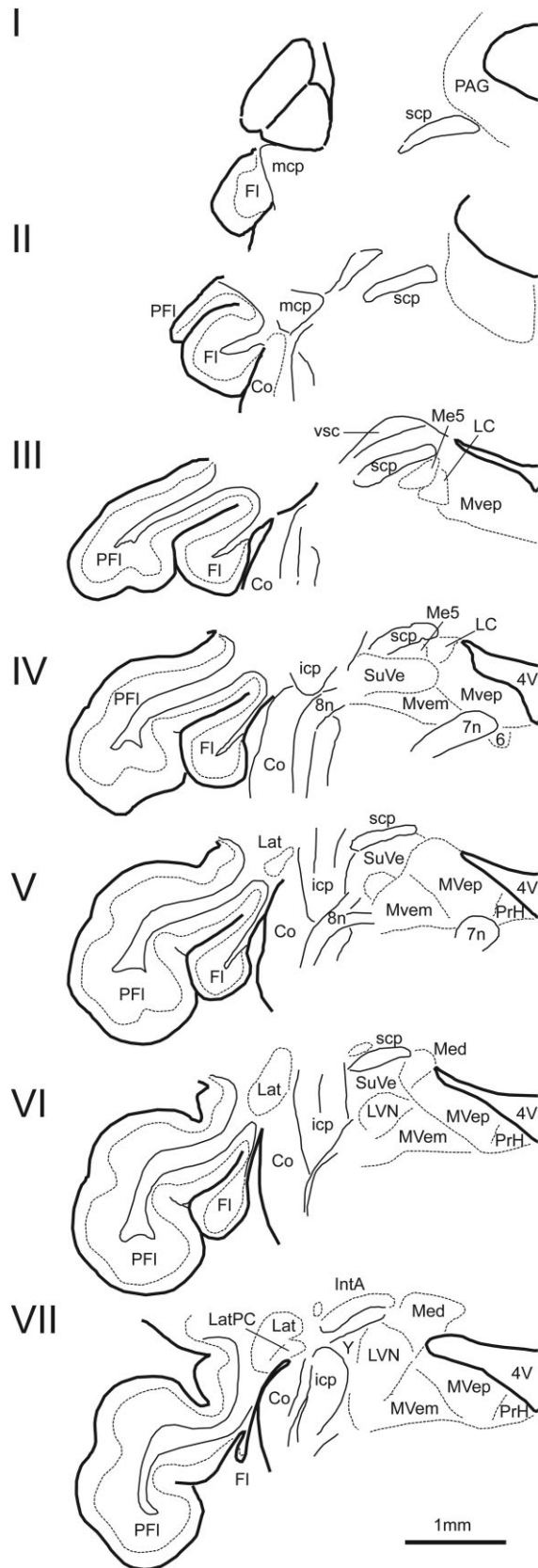
the left flocculus. (B) Sinusoidal optokinetic stimulation was presented at 0.4 Hz. (C) Examples of peristimulus time histograms of complex spike activity of two Purkinje cells showing an optimal response to HA (left) or VA (right) optokinetic stimulation. (D) As in C but for simple spikes; note reciprocal modulation in that increased simple spike activity is accompanied by decreased complex spike activity and vice versa. The histograms in C and D show the average firing frequency over 40 cycles per bin (bin width is 25 milliseconds).

the Purkinje cells that were located in the three most caudal zones, that is, zone C2, zone 1 and zone 2, were positively labeled for HSP-25 (Fig. 3B,C). In contrast, none of the Purkinje cells in zones 3 and 4 showed any immunoreactivity for HSP-25. In conjunction, these data indicate that the vast majority of Purkinje cells in the flocculus of the mouse respond to optokinetic stimulation about axes that run through the horizontal semicircular canal or ipsilateral anterior semicircular canal, that these cells are organized in parasagittal zones, and that they can be partly identified by immunohistochemical staining.

### Projections from the inferior olive to the flocculus

The data described above indicate that the complex spike activities of Purkinje cells in zones 1 and 3 modulate optimally around an axis that is perpendicular to the preferred axis of Purkinje cells in zones 2 and 4. These results suggest that the climbing fibers that evoke these

different activities originate from different clusters of neurons in the inferior olive. We therefore investigated whether the BDA injections in zones 1 and 3 resulted in different sets of retrogradely labeled neurons than those in zones 2 and 4. This prediction did hold (Table 1). The injections of BDA in zones 1 and 3 resulted in labeled neurons in the contralateral ventrolateral outgrowth (VLO; Fig. 4), whereas those in zones 2 and 4 resulted in retrogradely labeled neurons in the contralateral caudal dorsal cap (CDC; Fig. 5). In all cases the injections were relatively small and the number of retrogradely labeled neurons never exceeded 15. In 1 case, mouse 15735-5, the cluster of retrogradely labeled neurons in the caudal dorsal cap extended into a more rostral area approaching the rostral dorsal cap and VLO. Note that the injection site in this case was located near the border between zones 2 and 3 (Fig. 3D). In 3 cases we did not observe any retrogradely labeled neuron in the inferior olive (Table 1). Thus, collectively from these results we conclude that the sources of the climbing fiber projections to the different floccular



zones in the mouse are compatible with the preferred complex spike modulations of their Purkinje cells. The climbing fiber projections to both HA zones (1 and 3) are derived from the same olivary subnucleus, the VLO, while those to the VA zones (2 and 4) are both derived from a different subnucleus, the caudal dorsal cap (DC).

### Purkinje cell projections

The specific climbing fiber inputs as well as the preferred complex spike and simple spike modulations of the Purkinje cell zones described above would theoretically be most effective were it maintained in the nuclei receiving Purkinje cell inputs as well. We therefore investigated whether the BDA injections in the flocculus that provided the zone-specific retrograde labeling in the different olivary subnuclei, also showed anatomically discrete anterograde labeling of Purkinje cell axons and terminals.

The injections into the HA zones 1 and 3 demonstrated similar, yet not identical, projection patterns. Labeled fibers originating from zone 1 followed the floccular peduncle from which they turned caudally towards the parvicellular aspect of the lateral cerebellar nucleus (LatPC) where a dense axonal terminal plexus was observed in a confined narrow region (Figs. 4C and 6A). Other fibers followed an arching route through the LatPC passing just dorsal to the inferior cerebellar peduncle and Y-nucleus. At that point the fibers turned rostromedially and reached the superior vestibular nucleus (SuVe) where a few fibers and terminals were found. The fibers of zone 3 followed the same route as the fibers of zone 1, but they provided more terminal boutons in the SuVe and showed terminals in the dorsal part of group Y instead of the LatPC (Fig. 5).

The injections into VA zones 2 and 4 demonstrated projection patterns that clearly diverged from those of zones 1 and 3 (Table 1). Purkinje cell axons derived from zone 2 coursed ventrally to the LatPC and passed group Y without providing terminals to these regions. They descended ventromedially to terminate within the magnocellular and parvicellular parts of the medial vestibular nucleus (MVem and MVep). Occasionally, terminals were observed within the lateral vestibular nucleus (LVN) and sparsely in the nucleus prepositus hypoglossi (PrH; nr. 17770-1; Fig. 6F). Axon terminals were observed in all these regions, but the terminal arborizations were much more extensive in the MVem and MVep than in the LVN or PrH. Within the MVem many labeled terminals were distributed around large somata and proximal dendrites (Fig. 6G). In the case in which the injection site was close to the border with zone 3 (nr. 15735-5), some of the fibers also projected to the SuVe. The labeled Purkinje cell axons derived from zone 4 demonstrated a similar pattern of terminal arborizations as those of zone 2; most labeling was observed in the MVem and MVep, some in the LVN, and no axonal varicosities were seen within the confines of the LatPC or group Y.

Fig. 2. Series of drawings indicating the position and shape of the flocculus and paraflocculus in relation to the cerebellar and vestibular nuclei. Drawings were based on every fifth 40- $\mu$ m section of mouse 15733-2, and display the entire flocculus from its most rostral tip (I) down to its most caudal tip (VII). For abbreviations, see list.

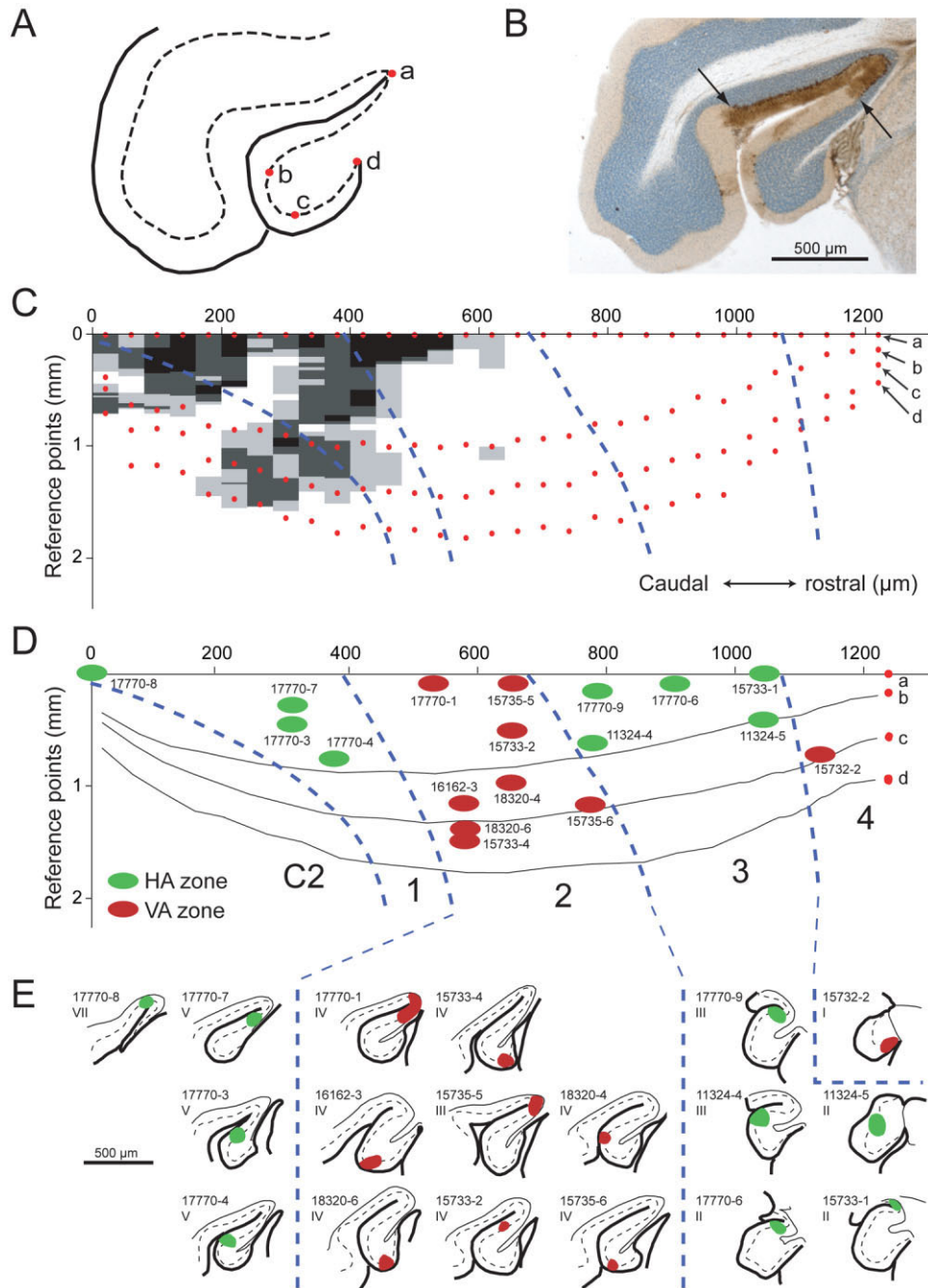


Fig. 3. The flocculus of the mouse can be divided into five functional zones. (A) Schematic representation of the flocculus showing the four reference points (a, b, c, and d) used in each floccular section (40  $\mu$ m) for analysis. (B) This panel illustrates an example of HSP-25 staining (brown) in the (para)flocculus (borders of the HSP-25-immunopositive area are indicated by arrows). (C) Schematic representation showing the HSP-25 expression pattern (from gray to black in increasing intensity) in the flocculus of the mouse with reference points a–d unfolded along the y-axis and consecutive sections presented in the rostrocaudal direction along the x-axis. Blue lines indi-

cate the borders of the functional zones identified by electrophysiological recordings. (D) This panel shows the BDA injection sites in HA (green) and VA (red) zones superimposed on the scheme presented in C. The numbers refer to the animals involved. Note that HSP-25 labeling is restricted to zones 1, 2, and C2. (E) Plots of original sections indicating the size and position of the BDA injections of all studied cases. Case numbers are indicated and Roman numbers refer to the approximate level of the plot relative to the series shown in Figure 2.

These data allow us to conclude that the Purkinje cell projections from HA zones (1 and 3) diverge from those of VA zones (2 and 4) and that the specifics of these

projection patterns match remarkably well with the characteristics of the climbing fiber inputs described above.

TABLE 1. List of Mice: Complex Spike Responses to HA or VA Optokinetic Stimulations, Injection, Projection Sites of BDA-Labeled Floccular Purkinje Cells, and Retrogradely Labeled Neurons in the Contralateral Inferior Olive

Mouse	Physiology	Zone	Ipsilateral Projection	Contralateral Inferior Olive
17770-3	HA	1	LatPC, SuVe	No labeling
17770-4	HA	1	LatPC, SuVe	VLO
17770-7	HA	1	LatPC, SuVe	VLO
17770-8	HA	1	No projection	VLO
18320-4	VA	2	No projection	CDC
15735-6	VA	2	MVep, some in LVN	No labeling
15733-4	VA	2	MVep, MVem, some in LVN	CDC
18320-6	VA	2	MVep, MVem	CDC
15733-2	VA	2	No projection	No labeling
17770-1	VA	2	MVem, MVep, some in PrH	CDC
16162-3	VA	2	MVep	CDC
15735-5	VA	2	SuVe and MVem, MVep	CDC
11324-4	HA	3	SuVe and MVep, group Y	VLO
15733-1	HA	3	group Y	VLO
11324-5	HA	3	SuVe, group Y	VLO
17770-6	HA	3	SuVe, group Y	VLO
17770-9	HA	3	SuVe, group Y	VLO
15732-2	VA	4	MVem, MVep, some in LVN	CDC

CDC, caudal dorsal cap; LatPC, parvicellular part of lateral cerebellar nucleus; MVem, magnocellular part of medial vestibular nucleus; MVep, parvicellular part of medial vestibular nucleus; PrH, nucleus prepositus hypoglossi; SuVe, superior vestibular nucleus; VLO, ventrolateral outgrowth.

## DISCUSSION

In the present study, for the first time, we demonstrated that subpopulations of Purkinje cells reside in anatomically and physiologically discrete zones in the mouse flocculus. In addition, we have shown that the individual zones of Purkinje cells receive climbing fiber inputs from different regions of the inferior olive and project to different sets of nuclei and subnuclei, thereby retaining structural and functional separation at all three levels of the cerebellar modules.

### Zones in the mouse flocculus

The mouse flocculus was found to have four parasagittal zones that responded to optokinetic stimulation about particular axes in space (zones 1 to 4) and one zone that was nonresponsive to optokinetic stimulation (C2 zone). Zones 1 and 3 contained Purkinje cells responding optimally to visual field rotation around the 45° contralateral azimuth/135° ipsilateral azimuth HA, while Purkinje cells located in zones 2 and 4 showed a maximal response to rotation around the VA. These data agree with the divisions that have been found in the rabbit flocculus following both zone-specific recordings and zone-specific stimulations. De Zeeuw and colleagues (De Zeeuw et al., 1994a) showed a near-identical organization of zones in the rabbit flocculus following recordings of complex spike and simple spike activities, while Van der Steen and colleagues (Van der Steen et al., 1994) were able to evoke binocular eye movements about the same HA and VA axes in space by electrical microstimulation of the corresponding zones. In these studies the sites of the recordings or stimulations were marked by a tracer and/or electrical lesion and subsequently correlated to anatomical zones, the borders of which were visualized with the use of acetylcholinesterase (AChE; Tan et al., 1995b). In mice, however, neither AChE nor any other biochemical marker tested to date clearly labels the borders between the zones in the vestibulocerebellum (De Zeeuw et al., 2004). However, Armstrong and colleagues have recently made note of HSP-25 patterning in the vestibulocerebellum (Armstrong

et al., 2000). Therefore, we tested the usefulness of HSP-25 as a morphological marker for zonal borders and found that this protein is expressed by Purkinje cells in HA zone 1, VA zone 2, and the non-HA / non-VA zone C2, but not by those in zones 3 and 4. Thus, although we have not been able to find a specific morphological marker for either the VA zones or HA zones, we did find a marker to segregate the two most rostral zones from the three caudal zones in mice.

The most rostral floccular VA zone (zone 4), which we have found both in mice and rabbits, has not been described for the cat at the physiological level. Sato and Kawasaki (1984) found three zones in the flocculus of the cat following electrical stimulation; stimulation of a caudal zone produced downward eye movements, while stimulation of a middle and rostral zone produced ipsilateral horizontal and upward eye movements, respectively. Thus, the organization of these zones suggests that the caudal zone of the cat flocculus corresponds to zone 1 of the mouse flocculus, the middle zone to zone 2 and the rostral zone to zone 3. It appears likely though that the cat flocculus also has a rostral VA zone, because it can be found at the anatomical level following anterograde tracing of its climbing fibers (Gerrits and Voogd, 1982). Possibly, the rostral VA zone was missed in the physiological study in the cat, because it is too narrow to be reliably detected by electrical stimulation. In support of this point, it should be noted that in rabbits too zone 4 could not be detected by electrical stimulation (Van der Steen et al., 1994), while it was evident following single unit recordings of modulating Purkinje cells (De Zeeuw et al., 1994a).

Similarly, Gerrits and Voogd (Gerrits, 1985) found the existence of the C2 zone in the cat flocculus based on its three-dimensional structure, its relation with adjacent cerebellar structures, and its connections. Presumably the cat C2 zone is like that in mice and rabbits in that it is not directly involved in the optokinetic reflex. The function of the C2 zone could be related to head movements, as stimulation of this zone in the flocculus evokes short-latency head movements (De Zeeuw and Koekkoek, 1997).

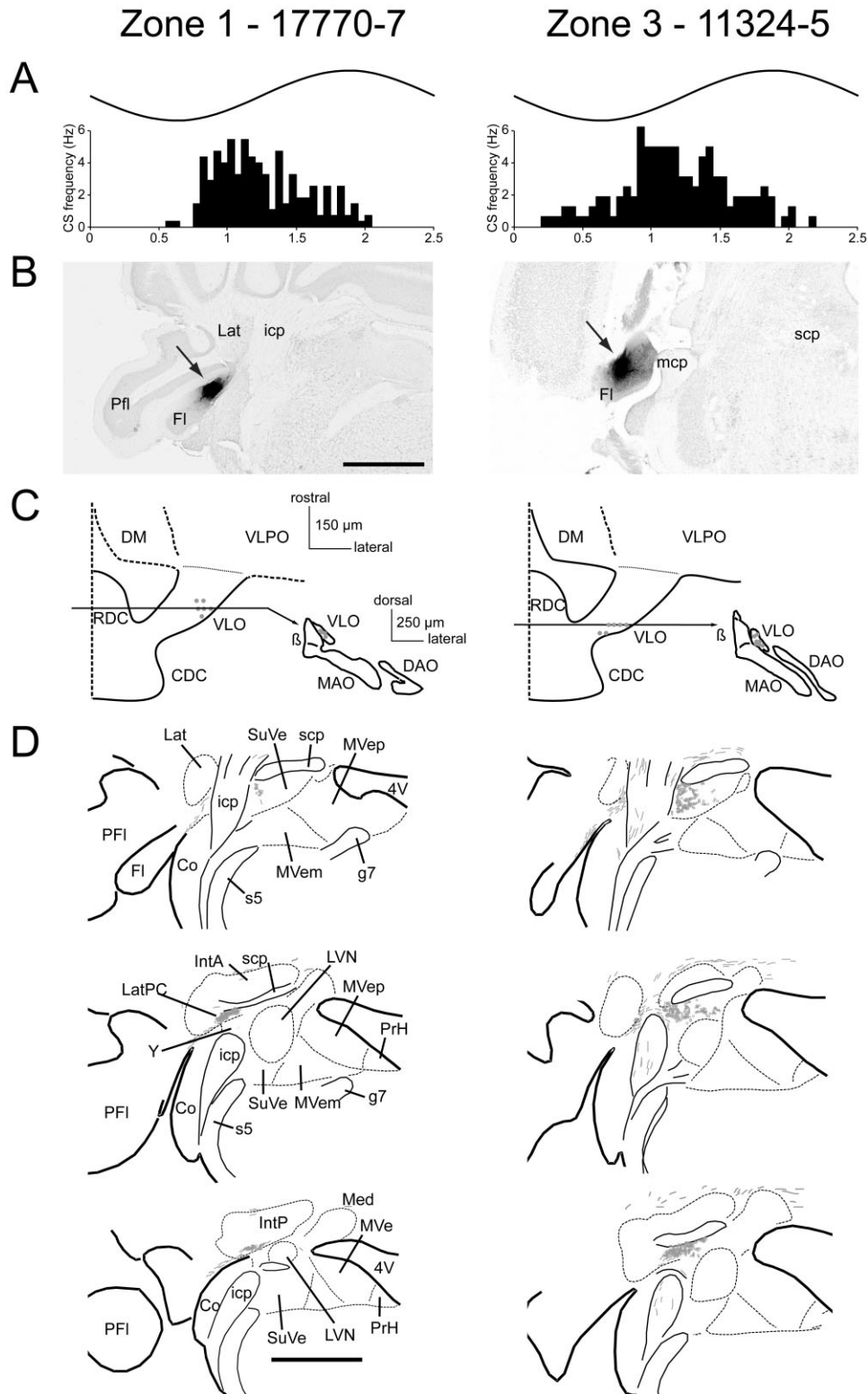


Fig. 4. Floccular zones 1 and 3, responding optimally to HA optokinetic stimulation, receive specific climbing fiber inputs and project to discrete regions in the midbrain. (A) Peri stimulus time histogram of the complex spikes modulation (bottom) demonstrating the response to sinusoidal HA stimulation (top). (B) Micrographs showing examples of BDA injection sites in zones 1 and 3 in the mouse flocculus. (C) Reconstructions of corresponding retrograde labeling in the contralateral inferior olive illustrate that the injections in zones 1

and 3 labeled olivary neurons (dots) in the ventrolateral outgrowth (VLO). Insets show a reconstruction of the coronal view at the rostrocaudal level indicated by the line. (D) Reconstructions of corresponding projection patterns shows that the injection in zone 1 resulted in Purkinje cells projecting to LatPC and SuVe, while the injection in zone 3 resulted in Purkinje cells projecting to group Y and SuVe. For abbreviations, see list.

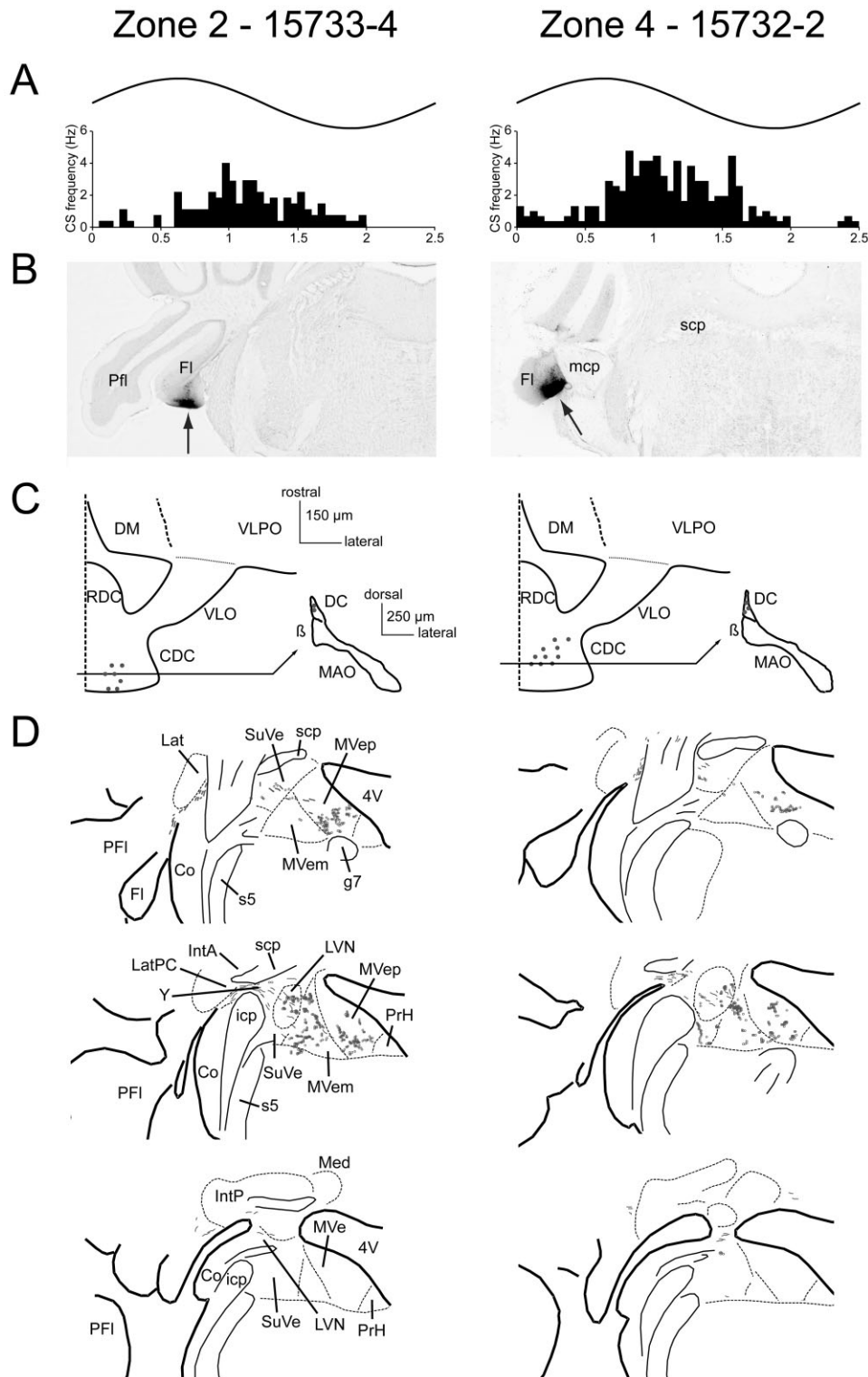


Fig. 5. Floccular zones 2 and 4, responding optimally to VA optokinetic stimulation, receive specific climbing fiber inputs and project to discrete regions in the midbrain. (A) Peri stimulus time histogram of the complex spikes modulation (bottom) demonstrating the response to sinusoidal VA stimulation (top). (B) Micrographs showing examples of BDA injection sites in zones 2 and 4 in the mouse flocculus. (C) Reconstructions of corresponding retrograde labeling in the contralateral inferior olive illustrate that the injections in zone 2

and 4 labeled olivary neurons (dots) in the caudal dorsal cap (CDC). Insets show a reconstruction of the coronal view at the rostrocaudal level indicated by the line. (D) Reconstructions of corresponding projection patterns shows that the injection in zones 2 and 4 (VA) resulted in Purkinje cells projecting to MVem and MVep, and in some cases to lesser extend also to the LVN or PrH. For abbreviations, see list.

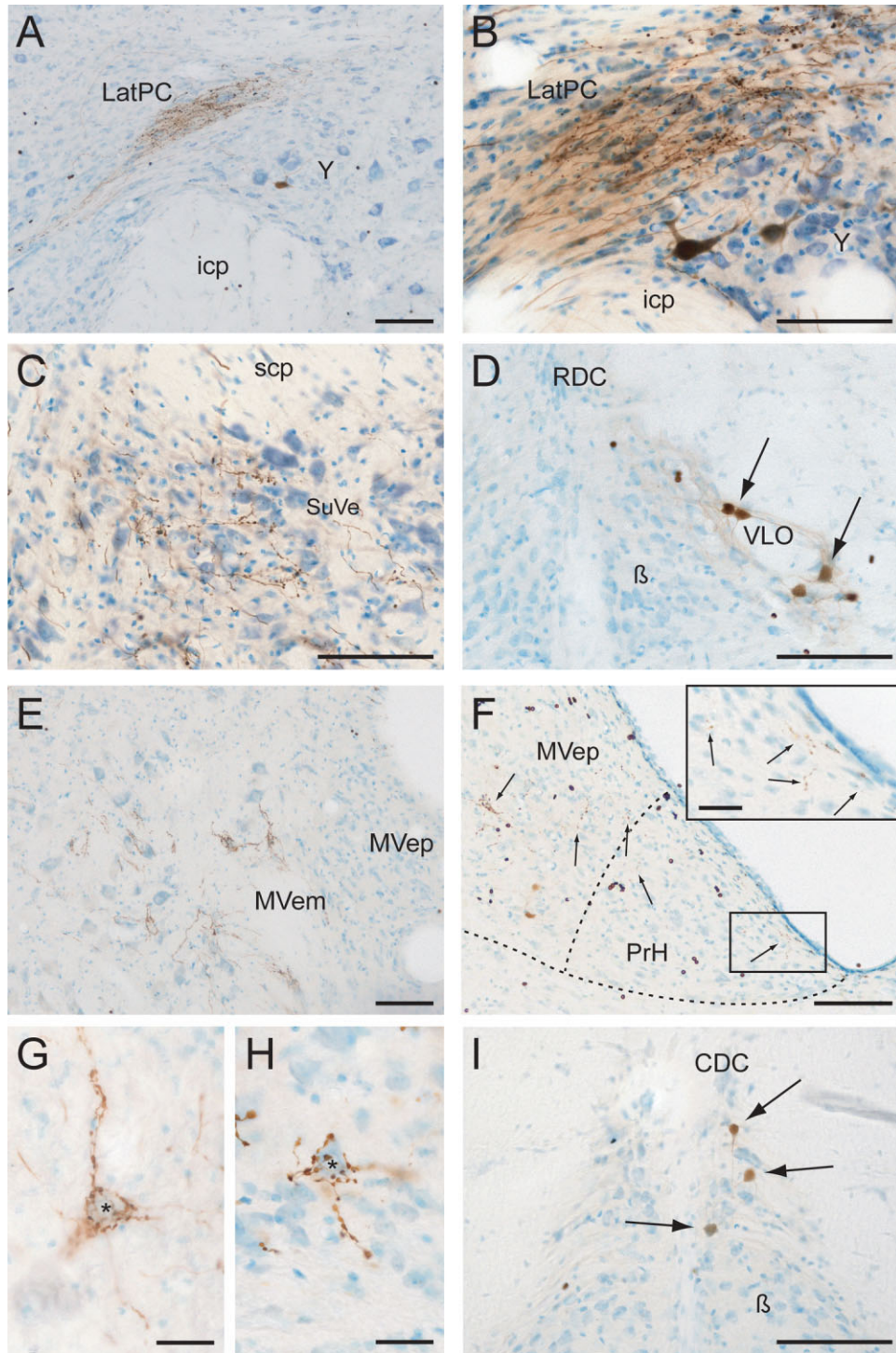


Fig. 6. Micrographs showing labeling characteristics after BDA injections into identified zones of the mouse flocculus. (A) Anterograde labeling of Purkinje cell axons and terminals within the LatPC following injection in zone 1 (case 17770-7). (B) Purkinje cell terminal arborizations are labeled within LatPC and group Y after BDA injection in zone 3 (case 11324-5). (C) Same case also shows efferent labeling within the lateral part of the SuVe. (D) Retrograde labeled neurons (arrows) are present in the VLO after BDA injection in zone 3 of the contralateral flocculus (case 17770-6). (E) Varicose fibers and terminals in the MVem are labeled after injection into zone 2 of the

flocculus (case 15733-4). (F) Anterograde labeling of Purkinje cell axons and terminals within the PrH following injection in zone 2 (case 17770-1). (G, H) These panels show examples of vestibular nucleus neurons (asterisks) that are surrounded by labeled terminal fibers after BDA injections into zone 2 (case 15733-4) and zone 4 (case 15732-2), respectively. (I) Retrograde labeling of olivary neurons (arrows) in the CDC after BDA injection into zone 4 of the flocculus (case 15732-2). Scale bars represent 25  $\mu$ m in G, H, and inset of F, and 100  $\mu$ m in all other panels. For abbreviations, see list.

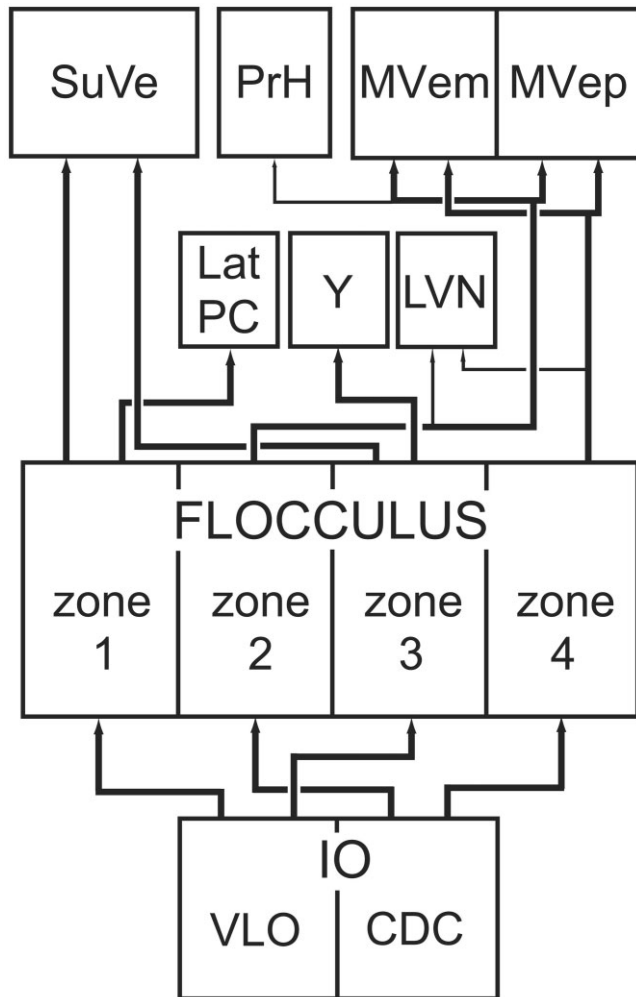


Fig. 7. Summary of afferent and efferent pathways of Purkinje cells in the mouse flocculus. Line width indicates the relative strength of the projection. For abbreviations, see list.

### Climbing fiber input to the mouse flocculus

The observation that complex spike activities in the mouse flocculus can be divided into discrete zones based on their responses to optokinetic stimulation around particular axes in space agreed well with the finding that these zones receive their climbing fiber inputs from different olivary subnuclei. We showed that Purkinje cells in HA zones 1 and 3 receive their climbing fibers from the VLO, while those in VA zones 2 and 4 receive their climbing fibers from the caudal DC. These data largely agree with the findings by Tan and colleagues (Tan et al., 1995c) in rabbit, except that zones 1 and 3 in that species also receive inputs from the rostral DC. The zonal organization of the olivocerebellar projection to the flocculus in the mouse also shows a pattern similar to that in the rat (Ruigrok et al., 1992; Sugihara et al., 2004); zones FD and FD' in the rat correspond to zones 1 and 3 and are innervated by the VLO, while zones FE and FE' are innervated by the dorsal cap and correspond to zone 2 and zone 4, respectively. Thus, one can conclude that the VLO and

caudal DC in animals in the grandorder glires are generally involved in vertical and horizontal optokinetic eye movements, respectively, and that the olivary projections to the flocculus in the mouse resemble those that have been described for rats and rabbits.

### Purkinje cell projections of the mouse flocculus

The organization of the output of the flocculus in mice was as zone-specific as that of its climbing fiber input and its Purkinje cell activities. Our findings reveal that Purkinje cells of zone 1 project to the LatPC and/or SuVe, that Purkinje cells of zone 3 project to group Y and/or SuVe, and that those of zone 2 and 4 project to the MVem and MVep, and occasionally to the LVN and PrH. These results largely agree with degeneration and tracing studies in rabbits (Yamamoto et al., 1978; Yamamoto, 1979; De Zeeuw et al., 1994a; Tan et al., 1995a), cats (Voogd, 1964; Sato et al., 1982a,b; Carleton and Carpenter, 1983; Dietrichs, 1983; Langer et al., 1985), monkeys (Balaban et al., 1981; Carleton and Carpenter, 1983; Langer et al., 1985), and rats (Bernard, 1987; Umetani, 1992; Balaban et al., 2000). The present study indicates that cells in the VA zone 2 project directly to neurons in the PrH. However, this projection was only clearly seen in case 17770-1 (Table 1), where the injection involved the medial part of the ventral paraflocculus. Purkinje cells in this area have been reported to be in labeled after injection in the PrH (Balaban et al., 2000). A projection from the flocculus to the PrH has been suggested before in the rabbit (Yamamoto et al., 1978), but De Zeeuw and colleagues (1994a) were unable to confirm this, let alone to determine from which zone it was derived. In addition, we observed a projection from zone 3, but not zone 1, to group Y in mice, while in rabbits both zones have been found to project to the dorsal part of group Y (De Zeeuw et al., 1994a). Thus, there may be subtle differences between mice and other mammals, but the main topographical organization appears very similar.

The results of this study in mice are comparable to previous studies in that there are 4 floccular zones for 2 preferred axes of optokinetic stimulation. These findings raise the question as to why there are 2 functional zones for each axis. A possible explanation may be found in the relatively subtle differences in the projections within the sets of HA zones and VA zones. For example, while Purkinje cells of zone 1 and zone 3 receive input from the same part of the inferior olive and respond both optimally to the same HA axis of optokinetic stimulation, the Purkinje cells in zone 1 project to the SuVe and LatPC whereas those in zone 3 project to the SuVe and the dorsal part of group Y. In all animals studied so far the LatPC is known to provide an inhibitory feedback to the inferior olive (De Zeeuw et al., 1994b), but whether this connection also holds for group Y is less clear (Partsalis et al., 1995). Similarly, the Purkinje cells in zone 2 may be involved in an inhibitory feedback to the olive via the PrH (De Zeeuw et al., 1993), but such projection has never been shown for zone 4. Thus, it appears possible that Purkinje cells zones 1 and 2 may be especially relevant for the closed loop systems in optokinetic control, while those of zones 3 and 4 may be more relevant for the open loop pathways (see also De Zeeuw et al., 1994a).

Finally, the current study provides the first direct evidence for mammals that the specific output connections of

the floccular zones perfectly match their specific climbing fiber inputs. We have been able to directly show this relation by combining anterograde and retrograde transport of a single tracer, BDA. Fortunately, the speed and efficiency of the anterograde and retrograde transport of BDA were sufficiently comparable to allow us to identify both labeled neurons in the inferior olive and sites of Purkinje cell terminations in the cerebellar and vestibular nuclei in single sections following single injections. Whenever the source of the climbing fibers was not discrete, for example, when an injection site was close to the border between two zones, the Purkinje cell projections were similarly more diffuse. Therefore, the current data allow us to conclude that the olivocerebellar modules as originally described by Voogd and colleagues (Voogd and Glickstein, 1998) hold valid and reach an extremely high level of precise topography.

### ACKNOWLEDGMENTS

We thank E. Dalm and Ir. J. v.d. Burg for their excellent assistance.

### LITERATURE CITED

- Alley K. 1977. Anatomical basis for interaction between cerebellar flocculus and brainstem. In: Baker R, Berthoz A, editors. Control of gaze by brainstem neurons. Amsterdam: Elsevier. pp 109–117.
- Armstrong CL, Krueger-Naug AM, Currie RW, Hawkes R. 2000. Constitutive expression of the 25-kDa heat shock protein Hsp25 reveals novel parasagittal bands of purkinje cells in the adult mouse cerebellar cortex. *J Comp Neurol* 416:383–397.
- Balaban CD. 1987. Distribution of inferior olivary projections to the vestibular nuclei of albino rabbits. *Neuroscience* 24:119–134.
- Balaban CD, Ito M, Watanabe E. 1981. Demonstration of zonal projections from the cerebellar flocculus to vestibular nuclei in monkeys (*Macaca fuscata*). *Neurosci Lett* 27:101–105.
- Balaban CD, Schuergler RJ, Porter JD. 2000. Zonal organization of flocculo-vestibular connections in rats. *Neuroscience* 99:669–682.
- Bernard JF. 1987. Topographical organization of olivocerebellar and corticonuclear connections in the rat — an WGA-HRP study: I. Lobules IX, X, and the flocculus. *J Comp Neurol* 263:241–258.
- Carleton SC, Carpenter MB. 1983. Afferent and efferent connections of the medial, inferior and lateral vestibular nuclei in the cat and monkey. *Brain Res* 278:29–51.
- De Zeeuw CI, Koekkoek SKE. 1997. Signal processing in the C2-module of the flocculus and its role in head movement control. In: De Zeeuw, Strata, and Voogd, editors. The cerebellum from structure to control. Rotterdam: Elsevier. pp 299–320.
- De Zeeuw CI, Koekkoek SK, van Alphen AM, Luo C, Hoebeek F, van der Steen J, Frens MA, Sun JC, Goossens HHL, Jaarsma D, Coesmans MPH, Schmolesky MT, de Jeu MTG, Galjart N. 2004. Gain and phase control of compensatory eye movements by the flocculus of the vestibulo-cerebellum. In: Handbook of auditory research. New York: Springer-Verlag. pp 375–422.
- De Zeeuw CI, Wentzel P, Mugnaini E. 1993. Fine structure of the dorsal cap of the inferior olive and its GABAergic and non-GABAergic input from the nucleus prepositus hypoglossi in rat and rabbit. *J Comp Neurol* 327:63–82.
- De Zeeuw CI, Wylie DR, DiGiorgi PL, Simpson JI. 1994a. Projections of individual Purkinje cells of identified zones in the flocculus to the vestibular and cerebellar nuclei in the rabbit. *J Comp Neurol* 349:428–447.
- De Zeeuw CI, Gerrits NM, Voogd J, Leonard CS, Simpson JI. 1994b. The rostral dorsal cap and ventrolateral outgrowth of the rabbit inferior olive receive a GABAergic input from dorsal group Y and the ventral dentate nucleus. *J Comp Neurol* 341:420–432.
- Dieterichs E. 1983. The cerebellar corticonuclear and nucleocortical projections in the cat as studied with anterograde and retrograde transport of horseradish peroxidase. V. The posterior lobe vermis and the flocculonodular lobe. *Anat Embryol* 167:449–462.
- Eccles JC, Sasaki K, Strata P. 1966. The profiles of physiological events produced by a parallel fibre volley in the cerebellar cortex. *Exp Brain Res* 2:18–34.
- Gerrits NM. 1985. Brainstem control of the cerebellar flocculus. Leiden: Leiden University. P 1–89.
- Gerrits NM, Voogd J. 1982. The climbing fiber projection to the flocculus and adjacent paraflocculus in the cat. *Neuroscience* 7:2971–2991.
- Goossens HH, Hoebeek FE, Van Alphen AM, Van Der Steen J, Stahl JS, De Zeeuw CI, Frens MA. 2004. Simple spike and complex spike activity of floccular Purkinje cells during the optokinetic reflex in mice lacking cerebellar long-term depression. *Eur J Neurosci* 19:687–697.
- Goossens J, Daniel H, Rancillac A, van der Steen J, Oberdick J, Crepel F, De Zeeuw CI, Frens MA. 2001. Expression of protein kinase C inhibitor blocks cerebellar long-term depression without affecting Purkinje cell excitability in alert mice. *J Neurosci* 21:5813–5823.
- Graf W, Simpson JI, Leonard CS. 1988. Spatial organization of visual messages of the rabbit's cerebellar flocculus. II. Complex and simple spike responses of Purkinje cells. *J Neurophysiol* 60:2091–2121.
- Groenewegen HJ, Voogd J. 1977. The parasagittal zonation within the olivocerebellar projection. I. Climbing fiber distribution in the vermis of cat cerebellum. *J Comp Neurol* 174:417–488.
- Groenewegen HJ, Voogd J, Freedman SL. 1979. The parasagittal zonation within the olivocerebellar projection. II. Climbing fiber distribution in the intermediate and hemispheric parts of cat cerebellum. *J Comp Neurol* 183:551–601.
- Haines DE. 1977. Cerebellar corticonuclear and corticovestibular fibers of the flocculonodular lobe in a prosimian primate (*Galago senegalensis*). *J Comp Neurol* 174:607–630.
- Hoebeek FE, Stahl JS, van Alphen AM, Schonewille M, Luo C, Rutteman M, van den Maagdenberg AM, Molenaar PC, Goossens HH, Frens MA, De Zeeuw CI. 2005. Increased noise level of purkinje cell activities minimizes impact of their modulation during sensorimotor control. *Neuron* 45:953–965.
- Langer T, Fuchs AF, Chubb MC, Scudder CA, Lisberger SG. 1985. Floccular efferents in the rhesus macaque as revealed by autoradiography and horseradish peroxidase. *J Comp Neurol* 235:26–37.
- Lisberger SG, Fuchs AF. 1978. Role of primate flocculus during rapid behavioral modification of vestibuloocular reflex. II. Mossy fiber firing patterns during horizontal head rotation and eye movement. *J Neurophysiol* 41:764–777.
- Maatkamp A, Vluga A, Haasdijk E, Troost D, French PJ, Jaarsma D. 2004. Decrease of Hsp25 protein expression precedes degeneration of motoneurons in ALS-SOD1 mice. *Eur J Neurosci* 20:14–28.
- McCrea RA, Baker R, Delgado-Garcia J. 1979. Afferent and efferent organization of the prepositus hypoglossi nucleus. *Prog Brain Res* 50:653–665.
- Partsalis AM, Zhang Y, Highstein SM. 1995. Dorsal Y group in the squirrel monkey. I. Neuronal responses during rapid and long-term modifications of the vertical VOR. *J Neurophysiol* 73:615–631.
- Ruigrok TJ, Osse RJ, Voogd J. 1992. Organization of inferior olivary projections to the flocculus and ventral paraflocculus of the rat cerebellum. *J Comp Neurol* 316:129–150.
- Sato Y, Kawasaki T. 1984. Functional localization in the three floccular zones related to eye movement control in the cat. *Brain Res* 290:25–31.
- Sato Y, Kawasaki T, Ikarashi K. 1982a. Zonal organization of the floccular Purkinje cells projecting to the vestibular nucleus in cats. *Brain Res* 232:1–15.
- Sato Y, Kawasaki T, Ikarashi K. 1982b. Zonal organization of the floccular Purkinje cells projecting to the group y of the vestibular nuclear complex and the lateral cerebellar nucleus in cats. *Brain Res* 234:430–434.
- Stahl JS, van Alphen AM, De Zeeuw CI. 2000. A comparison of video and magnetic search coil recordings of mouse eye movements [In Process Citation]. *J Neurosci Methods* 99:101–110.
- Sugihara I, Ebata S, Shinoda Y. 2004. Functional compartmentalization in the flocculus and the ventral dentate and dorsal group y nuclei: an analysis of single olivocerebellar axonal morphology. *J Comp Neurol* 470:113–133.
- Tan J, Epema AH, Voogd J. 1995a. Zonal organization of the flocculo-vestibular nucleus projection in the rabbit: a combined axonal tracing and acetylcholinesterase histochemical study. *J Comp Neurol* 356:51–71.
- Tan J, Simpson JI, Voogd J. 1995b. Anatomical compartments in the white matter of the rabbit flocculus. *J Comp Neurol* 356:1–22.
- Tan J, Gerrits NM, Nanhoe R, Simpson JI, Voogd J. 1995c. Zonal organization of the climbing fiber projection to the flocculus and nodulus of

- the rabbit: a combined axonal tracing and acetylcholinesterase histochemical study. *J Comp Neurol* 356:23–50.
- Thach WT Jr. 1967. Somatosensory receptive fields of single units in cat cerebellar cortex. *J Neurophysiol* 30:675–696.
- Umetani T. 1992. Efferent projections from the flocculus in the albino rat as revealed by an autoradiographic orthograde tracing method. *Brain Res* 586:91–103.
- van Alphen AM, Stahl JS, De Zeeuw CI. 2001. The dynamic characteristics of the mouse horizontal vestibulo-ocular and optokinetic response. *Brain Res* 890:296–305.
- Van der Steen J, Simpson JI, Tan J. 1994. Functional and anatomic organization of three-dimensional eye movements in rabbit cerebellar flocculus. *J Neurophysiol* 72:31–46.
- Voogd J. 1964. The cerebellum of the cat. Structure and fibre connexions. In: *Anatomie*. Leiden: Ryks universiteit Leiden.
- Voogd J, Bigaré F. 1980. Topographical distribution of olivary and corticonuclear fibers in the cerebellum. The inferior olivary nucleus. Raven Press: New York. P. 207–305.
- Voogd J, Glickstein M. 1998. The anatomy of the cerebellum. *Trends Neurosci* 21:370–375.
- Yamamoto M. 1979. Topographical representation in rabbit cerebellar flocculus for various afferent inputs from the brainstem investigated by means of retrograde axonal transport of horseradish peroxidase. *Neurosci Lett* 12:29–34.
- Yamamoto M, Shimoyama I. 1977. Differential localization of rabbit's flocculus Purkinje cells projecting to the medial and superior vestibular nuclei, investigated by means of the HRP retrograde axonal transport. *Neuroscience* 5:279–283.
- Yamamoto M, Shimoyama I, Highstein SM. 1978. Vestibular nucleus neurons relaying excitation from the anterior canal to the oculomotor nucleus. *Brain Res* 148:31–42.